CEAI, Vol.24, No.1, pp. 45-56, 2022 Printed in Romania

Decoupled Adaptive Backstepping Sliding Mode Control of Underactuated Mechanical Systems

Baris Ata*, Ramazan Coban**

Cukurova University, Department of Computer Engineering, 01330 Balcali, Saricam, Adana, Turkey
*(*Tel:+903223387101x17; e-mail: bata@cu.edu.tr, **Tel:+903223387101x15; e-mail: rcoban@cu.edu.tr)*

Abstract: In this paper, a combination of sliding mode control and adaptive backstepping control with a decoupling algorithm is considered for controlling 2 degrees of freedom underactuated mechanical systems subject to parametric uncertainties and external disturbances. The stability of the system is assured by the design steps of the proposed decoupled adaptive backstepping sliding mode control which are based on the Lyapunov theorem. The effectiveness of the proposed decoupled adaptive backstepping sliding mode control method is compared against a decoupled sliding mode controller by testing on a real-life inverted pendulum on a cart system which is a classical testbed for underactuated mechanical systems. The experimental outcomes justify the proposed decoupled adaptive backstepping sliding mode controller provides a more satisfying performance compared to the conventional decoupled sliding mode controller. Besides the proposed method is able to handle parametric uncertainties contrarily to the decoupled sliding mode control.

Keywords: Decoupled sliding mode; Adaptive backstepping; Inverted pendulum on a cart; Underactuated mechanical systems

1. INTRODUCTION

The control of underactuated mechanical systems (UMSs) has been attracting great interest during the last decades (Fantoni and Lozano, 2002; Huang et al., 2019; Liu and Yu, 2013; Reyhanoglu et al., 1999; Spong, 1998). UMSs refer to the systems that have fewer actuators than the number of degrees of freedom (DOF). A system can become underactuated by the natural dynamics of the system, by design to reduce the cost, by artificially induced for a research purpose, or by actuator failure (Hussein and Bloch, 2008; Spong, 1987; Walsh et al., 1994). Separated from the cause of becoming underactuated, UMSs present some advantages including reduction of cost, energy, and complexity compared to fully actuated mechanical systems due to lower numbers of actuators. Therefore, UMSs are widely used in real-life applications like underwater vehicles, aerospace, and robotics (Olfati-Saber, 2001; Oryschuk et al., 2009; Woods et al., 2012). However, unlike the fully actuated mechanical systems, controlling UMSs presents a more challenging task because of their nonholonomic constraints (Isidori, 1995).

The inverted pendulum on a cart (IPC) system is a classical instance of UMSs. The IPC system consists of 2 DOF, both the cart position and the pendulum angle are controlled by a single actuator. Also, given its unstable and nonlinear nature, the IPC system has been a benchmark tool for testing various kinds of control techniques. Moreover, the dynamics of the IPC system are fundamental to the maintaining balance problem and resembles many real systems such as two-wheeled robots, bipedal walking, humanoid robots, and rocket thrusters (Anderson, 1988; Jeong and Takahashi, 2007; Kuo, 2007). Therefore, numerous control approaches such as energy-based control (Åström and Furuta, 2000; Siuka and Schöberl, 2009), PID control (Chang et al., 2002; Subudhi et al., 2012) linear quadratic regulator (Coban and Ata, 2017; Saco, 2019), backstepping (Deng and Gao, 2011) and sliding mode control (SMC) (Adhikary and Mahanta, 2013; Coban and Ata, 2017; Lo and Kuo, 1998; Mahjoub et al., 2015) have been suggested for controlling the IPC system.

As a robust control method, the SMC has been extensively used to control nonlinear systems (Slotine and Li, 1991; Utkin, 1977). The main advantages of the SMC contain fast response and robustness to external disturbances and model uncertainties (Utkin, 1992). The key idea of the SMC method is constructing a suitable sliding manifold that drives the trajectories to zero within it. The main drawback of the conventional SMC method is the high-frequency oscillation on the sliding surface known as the chattering phenomenon (Lee and Utkin, 2007). Also, the system has to be transformed into the canonical form to apply the conventional SMC method to UMSs. To handle this drawback, decoupled sliding mode control (DSMC) can be employed to control the UMSs (Coban and Ata, 2017; Lo and Kuo, 1998). Furthermore, the SMC technique can be combined with other control techniques such as backstepping and adaptive backstepping methods to handle parametric uncertainties (Ata and Coban, 2019; Coban, 2019; Lin et al., 2002).

The backstepping method is a robust control scheme based on the Lyapunov stability approach (Freeman and Kokotović, 1996; Kanellakopoulos et al., 1991). The backstepping approach provides a recursive procedure to dividing the control problem into a series of control problems for lower order subsystems and it is natural to combine the backstepping method with the SMC (Ma et al., 2006). Because of its robustness to disturbances and uncertainties, the backstepping sliding mode control (BSMC) is an active research area in recent years (Ata and Coban, 2019; Coban, 2019; Liu et al., 2020). However, determining the upper bound of external disturbances is a challenging task for designing the BSMC. To address this problem the adaptive backstepping sliding mode control (ABSMC) approach can be employed in controller design (Lin et al., 2002; Wu and Lu, 2019).

An adaptive backstepping sliding mode control approach for nonlinear uncertain systems is suggested in (Coban, 2019) to obtain a chattering-free control and overcome parametric and unstructured uncertainties. However, this method is designed for a second-order, single input–single output nonlinear electromechanical system and it cannot be directly applied to fourth-order underactuated nonlinear systems with single input and 2 DOF. A decoupled backstepping sliding mode control design method is proposed in (Ata and Coban, 2019) to control underactuated systems under uncertainties. Yet, this method needs prior knowledge of the upper bounds of uncertainties and disturbances. This paper presents a decoupled adaptive backstepping sliding mode control (DABSMC) approach to control 2 DOF UMSs subject to parametric uncertainties. The proposed method can be applied to UMSs directly due to its decoupling nature. Also, the proposed method removes the need for prior knowledge of the upper bounds of uncertainties on the decoupled backstepping sliding mode control design by employing an adaptive scheme. The proposed approach has been tested on a real IPC system to validate the effectiveness and performance of the DABSMC method for a class of UMSs. This class of UMSs is featured as a fourth-order underactuated nonlinear system with single input and 2 DOF. The proposed method will fail when it is applied to the systems higher than fourth-order as a consequence of the two-level control system model of the DSMC approach (Lo and Kuo, 1998).

The rest of the paper is structured as follows. Section 2 introduces the dynamics of the IPC system considered in the paper. In section 3, the ABSMC method is presented and the design procedure of the DABSMC approach is introduced. The proposed DABSMC and the conventional DSMC methods are compared and the experimental results are presented in section 4. Conclusions of the study are reported in section 5.

2. DYNAMICS OF THE IPC SYSTEM

The IPC system is a classical benchmark problem for UMSs. It consists of a cart and a pendulum that is attached to the cart as shown in Fig. 1. Therefore, the IPC system has 2 DOF; one for the horizontal movement of the cart and one for the angular movement of the pendulum. Only the horizontal motion of the cart is actuated in the IPC system. The rotational motion of the pendulum is indirectly controlled by the movement of the cart.

Consider the cart displacement from the initial position as x and the angular displacement of the pendulum from the vertical position as θ. Using the Euler-Lagrange method while including the effects of cart friction and pendulum damping, the equation of motions for horizontal motion and rotational motion can be derived as (Ata and Coban, 2017).

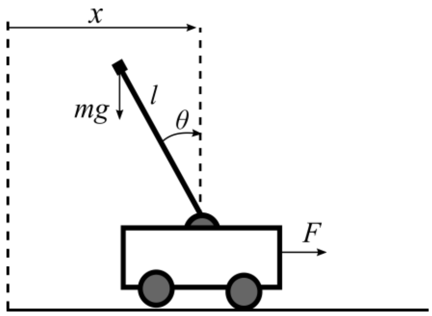

Fig. 1. Parametric representation of the IPC system.

$$\ddot{x} = \frac{-(I+ml^2)b\dot{x} + m^2l^2 g cos(\theta) sin(\theta)}{(I+ml^2)(M+m) - m^2l^2cos^2(\theta)} - \frac{mlcos(\theta)d\dot{\theta} + (I+ml^2)ml\dot{\theta}^2 sin(\theta) + (I+ml^2)F}{(I+ml^2)(M+m) - m^2l^2cos^2(\theta)} \tag{1}$$

and

$$\ddot{\theta} = \frac{(M+m)mglsin(\theta) - m^2l^2cos(\theta)sin(\theta)\dot{\theta}^2}{(I+ml^2)(M+m) - m^2l^2cos^2(\theta)} - \frac{mlbcos(\theta)\dot{x} + (M+m)d\dot{\theta} - mlcos(\theta)F}{(I+ml^2)(M+m) - m^2l^2cos^2(\theta)} \tag{2}$$

where M is the mass of the cart; b is the cart friction coefficient; l and m are the length and the mass of the pendulum, respectively; d is the pendulum damping coefficient; I is the moment of inertia; F represents the force applied to the cart as control action and g is the acceleration due to gravity.

Since the cart is actuated by a DC motor in real-life applications, adding the motor characteristics to the IPC system model will provide a more realistic system design (Kennedy et al., 2019). The input of the IPC system is equal to the DC motor voltage of the cart. The input voltage $v(t)$ is converted to driving force $F(t)$ according to the equation (Ata and Coban, 2017):

$$F(t) = -\frac{K_b K_t n_1 n_2}{R_m r_m^2}\dot{x}(t) + \frac{K_t n_1}{R_m r_m} v(t) \tag{3}$$

where K_b is the back-electromotive force constant; K_t is the motor torque constant; n_1 and n_2 are gear ratios; R_m is the motor armature resistance and r_m is the radius of the pulley.

Substituting the voltage-force conversion in (3) into equations of motions in (1) and (2) by defining the system states $[x_1\ x_2\ x_3\ x_4]^T$ as $[x\ \dot{x}\ \theta\ \dot{\theta}]^T$ and considering $u(t) = v(t)$, one can get the state equations of the IPC system as follows (Ata & Coban, 2019):

$$
\begin{aligned}
\dot{x}_1 &= x_2 \\
\dot{x}_2 &= \frac{\omega_1\left(a_{n1}x_2 + a_{n2}\cos(x_3)\sin(x_3) + a_{n3}\sin(x_3)x_4^2\right)}{a_{m1} - a_{m2}\cos^2(x_3)} \\
&\quad + \frac{\omega_1 a_{n4}\cos(x_3)x_4 + a_{n5}u}{a_{m1} - a_{m2}\cos^2(x_3)} + \varepsilon_1(t) \\
\dot{x}_3 &= x_4 \\
\dot{x}_4 &= \frac{\omega_2\left(a_{n6}x_2\cos(x_3) + a_{n7}\sin(x_3) + a_{n7}x_4\right)}{a_{m1} - a_{m2}\cos^2(x_3)} \\
&\quad + \frac{\omega_2 a_{n8}\cos(x_3)\sin(x_3)x_4^2 + a_{n9}\cos(x_3)u}{a_{m1} - a_{m2}\cos^2(x_3)} + \varepsilon_2(t)
\end{aligned}
\tag{4}
$$

where

$$
\begin{aligned}
a_{n1} &= -(I + ml^2)\left(b + (K_b K_t n_1 n_2)/(R_m r_m^2)\right) \\
a_{n2} &= m^2 l^2 g \\
a_{n3} &= -(I + ml^2)ml \\
a_{n4} &= -mld \\
a_{n4} &= (I + ml^2)\left(b + (K_t n_1)/(R_m r_m)\right) \\
a_{n5} &= -ml\left(b + (K_b K_t n_1 n_2)/(R_m r_m^2)\right) \\
a_{n6} &= (M + m)mgl \\
a_{n7} &= m^2 l^2 \\
a_{n8} &= (M + m)d \\
a_{n9} &= ml\left((K_t n_1)/(R_m r_m)\right) \\
a_{m1} &= (I + ml^2)(M + m) \\
a_{m2} &= m^2 l^2;
\end{aligned}
$$

$\varepsilon_1(t)$ and $\varepsilon_2(t)$ stand for the overall external disturbances and ω_1 and ω_2 are constants refer to the parametric uncertainties. $\varepsilon_1(t)$ and $\varepsilon_2(t)$ are considered to be bounded as $|\varepsilon_1(t)| \le \varepsilon_{1\max}$ and $|\varepsilon_2(t)| \le \varepsilon_{2\max}$.

3. DESIGN METHODS

In this section, the ABSMC method is presented and the design procedure of the DABSMC method for UMSs is introduced. The stability analysis of both methods is based on Lyapunov theory and sliding modes features.

3.1 Adaptive Backstepping Sliding Mode Control

The dynamic model of a second-order, single-input single-output nonlinear system considered further is:

$$
\begin{aligned}
\dot{x}_1(t) &= x_2(t) \\
\dot{x}_2(t) &= \phi(x,t) + \gamma(x,t)u(t) + \varepsilon(t) \\
y(t) &= x_1(t)
\end{aligned}
\tag{5}
$$

where $x = [x_1, x_2]^T$ is the state vector, $y(t)$ is the output, $\phi(x,t)$ and $\gamma(x,t)$ are nonlinear functions, $u(t)$ is the control input, and, $\varepsilon(t)$ is the total amounts of unmatched uncertainties and external disturbances.

The control objective is to design an ABSMC law to track the desired output $y_d(t)$. Assume that not only the desired output $y_d(t)$ but also its first two derivatives with respect to the time $\dot{y}_d(t)$, $\ddot{y}_d(t)$, are available and all bounded functions of time. To achieve the control objective, the tracking error can be considered as

$$
\begin{aligned}
z_1(t) &= y(t) - y_d(t) \\
&= x_1(t) - y_d(t).
\end{aligned}
\tag{6}
$$

The time derivative of the tracking error $z_1(t)$ results in

$$
\dot{z}_1(t) = x_2(t) - \dot{y}_d(t). \tag{7}
$$

Since the main idea of the backstepping is to use some of the state variables as virtual controls, $x_2(t)$ can be considered as a virtual control signal. The desired value of the virtual controller is called the stabilizing function in the backstepping design (Kristic et al., 1995). Defining a stabilizing function as

$$
\alpha_1(t) = c_1 z_1(t) \tag{8}
$$

where c_1 is a positive constant and considering $x_2(t) = z_2(t) + \dot{y}_d(t) - \alpha_1(t)$ as a virtual controller yield $z_2(t) = x_2(t) - \dot{y}_d(t) + \alpha_1(t)$ as illustrated in Fig. 2. Accordingly, the second-order nonlinear system in Fig. 2 can be written as

$$
\begin{aligned}
\dot{x}_1(t) &= \phi(x,t) + \gamma(x,t)z_2(t) + \varepsilon(t) \\
\dot{x}_2(t) &= u(t) \\
y(t) &= x_1(t).
\end{aligned}
$$

Also note that an intermediate variable can be defined as $\tilde{\alpha}_1(t) = \alpha_1(t) - \dot{y}_d(t)$ and this variable can step back through the integrator as shown in Fig. 3 (Kristic et al., 1995). This is why this control design technique is known as “backstepping”.

The first term of the Lyapunov function candidate can be selected as

$$
V_1(t) = \frac{1}{2}z_1^2(t) \tag{9}
$$

and the time derivative of $V_1(t)$ can be derived as

$$
\begin{aligned}
\dot{V}_1(t) &= z_1(t)\dot{z}_1(t) \\
&= z_1(t)\left(x_2(t) - \dot{y}_d(t)\right) \\
&= z_1(t)\left(z_2(t) - \alpha_1(t)\right) \\
&= z_1(t)z_2(t) - c_1 z_1^{\,2}(t).
\end{aligned}
\tag{10}
$$

In the next step, considering a switching function as

$$
\sigma(t) = k_1 z_1(t) + z_2(t) \tag{11}
$$

where k_1 is a positive constant, the Lyapunov function candidate can be expanded as

$$V_2(z) = V_1(z) + \frac{1}{2}\sigma^2(t). \tag{12}$$

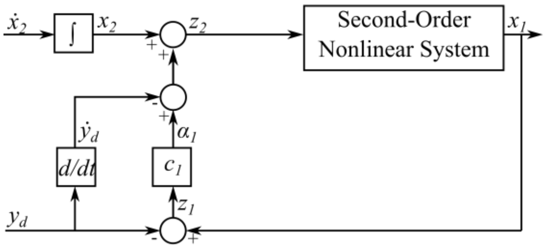

Fig. 2. Introducing the stabilizing function $\alpha_1(t)$ and the error variable $z_2(t)$.

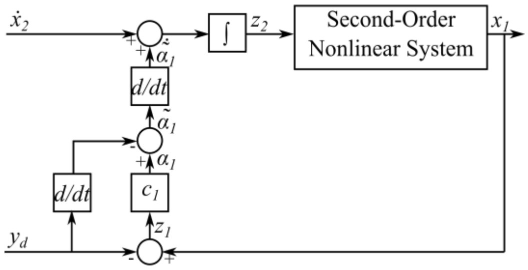

Fig. 3. Backstepping $\tilde{\alpha}_1(t)$ through the integrator.

By virtue of (5), the time derivative of $z_2(t)$ can be expressed as

$$\begin{aligned} \dot{z}_2(t) &= \dot{x}_2(t) - \ddot{y}_d(t) + \dot{\alpha}_1(t) \\ &= \phi(x,t) + \gamma(x,t)u(t) + \delta(t) - \ddot{y}_d(t) + \dot{\alpha}_1(t). \end{aligned} \tag{13}$$

Using (10) and (13), the time derivative of $V_2(z)$ can be derived as

$$\begin{aligned} \dot{V}_2(z) &= \dot{V}_1(z) + \sigma(t)\dot{\sigma}(t) \\ &= z_1(t)z_2(t) - c_1 z_1^2(t) + \sigma(t)\dot{\sigma}(t) \\ &= z_1(t)z_2(t) - c_1 z_1^2(t) + \sigma(t)\left[k_1\dot{z}_1(t) + \dot{z}_2(t)\right] \\ &= z_1(t)z_2(t) - c_1 z_1^2(t) + \sigma(t)\left[k_1\left(z_2(t) - c_1 z_1(t)\right)\right] \\ &\quad + \sigma(t)\left[\phi(x,t) + \gamma(x,t)u(t) + \delta(t) - \ddot{y}_d(t) + \dot{\alpha}_1(t)\right]. \end{aligned} \tag{14}$$

The BSMC law can be defined to assure that $V_2(z)$ is negative definite as follows (Lin et al., 2002):

$$\begin{aligned} u_{BS}(t) &= \frac{1}{\gamma(x,t)}\left[-k_1(z_2(t) - c_1 z_1(t)) - \phi(x,t) - \bar{\delta}(t) sgn(\sigma(t))\right] \\ &\quad + \frac{1}{\gamma(x,t)}\left[\ddot{y}_d(t) - \dot{\alpha}_1(t) - h\left(\sigma(t) + \beta sgn\left(\sigma(t)\right)\right)\right] \end{aligned} \tag{15}$$

where h and β are positive constants, the uncertainty $\delta(t)$ is assumed to be bounded $|\delta(t)| < \bar{\delta}(t)$, and, the signum function $sgn(\sigma(t))$ is

$$sgn(\sigma(t)) = \begin{cases} 1, & \sigma(t) > 0 \\ 0, & \sigma(t) = 0 \\ -1, & \sigma(t) < 0 \end{cases} \tag{16}$$

Using the control law proposed in (15), the derivative of the $V_2(z)$ can be rewritten as

$$\begin{aligned} \dot{V}_2(z) &= z_1(t)z_2(t) - c_1 z_1^2(t) - h\sigma^2(t) - h\beta|\sigma(t)| \\ &\quad + \delta(t)\sigma(t) - \bar{\delta}(t)|\sigma(t)| \\ &\le z_1(t)z_2(t) - c_1 z_1^2(t) - h\sigma^2(t) - h\beta|\sigma(t)| \\ &\quad + |\sigma(t)|\left(|\delta(t)| - \bar{\delta}(t)\right) \\ &\le z_1(t)z_2(t) - c_1 z_1^2(t) - h\sigma^2(t) - h\beta|\sigma(t)|. \end{aligned} \tag{17}$$

The derivative of the $V_2(z)$ in (17) may be rearranged as

$$\dot{V}_2(z) = -z^T Q z - h\beta|\sigma(t)| \le 0 \tag{18}$$

where $z^T = \begin{bmatrix} z_1 & z_2 \end{bmatrix}$ and Q is a symmetric matrix as

$$Q = \begin{bmatrix} c_1 + hk_1^2 & hk_1 - 1/2 \\ hk_1 - 1/2 & h \end{bmatrix}. \tag{19}$$

The symmetric matrix Q has to be positive definite to ensure that $\dot{V}_2(z)$ is negative (Coban, 2019). Sylvester's Theorem states that a sufficient and necessary criterion to guarantee a symmetric matrix Q to be positive definite is that all the principal minors of it have positive determinants (Ge et al., 2002). Selecting proper values for the constants h, c_1, and, k_1 guarantees that Q is positive definite:

$$\begin{aligned} |Q| &= h(c_1 + hk_1^2) - (hk_1 - 1/2)^2 \\ &= hc_1 + hk_1 - 1/4 > 0. \end{aligned} \tag{20}$$

According to Barbalat's lemma, defining $W(t) = -\dot{V}_2(z)$ can show $W(t)$ leans to 0 as $t \to \infty$ (Koshkouei and Zinober, 2000; Slotine and Li, 1991). Hence, z_1 and z_2 converge to 0 as $t \to \infty$. It indicates that $\lim_{t\to\infty} y(t) = y_d$ and $\lim_{t\to\infty} x(t) = \dot{y}_d$ (Lin et al., 2002). Therefore, the asymptotic stability of the BSMC system is ensured.

One of the important advantages of the BSMC method is insensitivity to the matched uncertainties. However, unmatched uncertainties generally exist in experimental environments. The uncertainty $\delta(t)$ is an unknown parameter and determining the upper bound of uncertainty $\bar{\delta}(t)$ is a challenging part of the BSMC design. To address this problem an adaptive mechanism can be combined with the BSMC method (Wu and Lu, 2019). In this approach, uncertainty has to be estimated and satisfied by an adaptive law to reach a robust tracking performance (Dong and Tang, 2014). Hence, an adaptive law can be used to adjust the uncertainty $\delta(t)$ (Lin et al., 2002):

$$\tilde{\epsilon}(t) = \epsilon(t) - \hat{\epsilon}(t) \tag{21}$$

and

$$\dot{\tilde{\epsilon}}(t) = \dot{\epsilon}(t) - \dot{\hat{\epsilon}}(t) = -\dot{\hat{\epsilon}}(t) \tag{22}$$

where $\hat{\epsilon}(t)$ is estimation and $\tilde{\epsilon}(t)$ is estimation error. Using the adaptive law, a new Lyapunov function candidate can be defined as

$$V_3(z) = V_2(z) + \frac{1}{2\xi}\tilde{\epsilon}^2(t) \tag{23}$$

where ξ is a positive constant. The time derivative of $V_3(z)$ can be derived with the help of (17) as

$$\begin{aligned}
\dot{V}_3(z) &= \dot{V}_2(z) + \frac{1}{\xi}\tilde{\epsilon}(t)\dot{\tilde{\epsilon}}(t) \\
&= z_1(t)z_2(t) - c_1 z_1^2(t) + \sigma(t)\left[k_1(z_2(t) - c_1 z_1(t))\right] \\
&\quad + \sigma(t)\left[\phi(x,t) + \gamma(x,t)u(t) + \epsilon(t) - \ddot{y}_d + \dot{\alpha}_1(t)\right] \\
&\quad - \frac{1}{\xi}\tilde{\epsilon}(t)\dot{\hat{\epsilon}}(t) \\
&= z_1(t)z_2(t) - c_1 z_1^2(t) + \sigma(t)\left[k_1(z_2(t) - c_1 z_1(t)\right] \\
&\quad + \sigma(t)\left[\phi(x,t) + \gamma(x,t)u(t) + \hat{\epsilon}(t) - \ddot{y}_d + \dot{\alpha}_1(t)\right] \\
&\quad - \frac{1}{\xi}\tilde{\epsilon}(t)\left(\dot{\hat{\epsilon}}(t) - \xi\sigma(t)\right).
\end{aligned} \tag{24}$$

Considering the adaptation law $\dot{\hat{\epsilon}}(t)$ as

$$\dot{\hat{\epsilon}}(t) = \xi\sigma(t), \tag{25}$$

an ABSMC law can be designed as follows (Lin et al., 2002)

$$\begin{aligned}
u_{ABS}(t) &= \frac{1}{\gamma(t)}\left[-k_1\left(z_2(t) - c_1 z_1(t)\right) - \phi(t) - \hat{\epsilon}(t) + \ddot{y}_d - \dot{\alpha}_1\right] \\
&\quad + \frac{1}{\gamma(t)}\left[-h\left(\sigma(t) + \beta sgn\left(\sigma(t)\right)\right)\right]
\end{aligned} \tag{26}$$

Substituting (26) in (24) yields

$$\dot{V}_3(z) = z_1(t)z_2(t) - c_1 z_1^2 - h\sigma^2(t) - h\beta\,|\,\sigma(t)\,|\,. \tag{27}$$

The derivative of the $V_3(z)$ may be rearranged as

$$\dot{V}_3(z) = -z^T Q_A z - h\beta\,|\,\sigma(t)\,| \leq 0 \tag{28}$$

where $z^T = \begin{bmatrix} z_1 & z_2 \end{bmatrix}$ and Q_A is a symmetric matrix as

$$Q_A = \begin{bmatrix} c_1 + hk_1^2 & hk_1 - 1/2 \\ hk_1 - 1/2 & h \end{bmatrix}. \tag{29}$$

Similar to (19), choosing proper values for the constants h, c_1, and, k_1 guarantees that all the determinants of principal minors of Q_A be positive. Hence, the symmetric matrix Q_A will be positive definite according to Sylvester's theorem. It indicates that the closed-loop system will be asymptotically stable by using the ABSMC according to Barbalat's lemma.

The design steps of the ABSMC approach are summarized in Fig. 4.

Input : **System states** $x_1(t)$ and $x_2(t)$;
System functions $\phi(t)$ and $\gamma(t)$;
External disturbance $\epsilon(t)$;
Desired output $y_d(t)$;
Controller parameters c_1, k_1, ξ, h and β
Output: The ABSMC output $u_{ABS}(t)$

$z_1(t) = x_1(t) - y_d(t)$
$\alpha_1(t) = c_1 z_1(t)$
$z_2(t) = x_2(t) - \dot{y}_d(t) + \alpha_1(t)$
$V_1(t) = \frac{1}{2}z_1^2(t)$
$\sigma(t) = k_1 z_1(t) + z_2(t)$
$V_2(z) = V_1(z) + \frac{1}{2}\sigma^2(t)$
$\tilde{\epsilon}(t) = \epsilon(t) - \hat{\epsilon}(t)$
$\dot{\tilde{\epsilon}}(t) = \dot{\epsilon}(t) - \dot{\hat{\epsilon}}(t) = -\dot{\hat{\epsilon}}(t)$
$V_3(z) = V_2(z) + \frac{1}{2\xi}\tilde{\epsilon}^2(t)$
$\dot{\hat{\epsilon}}(t) = \xi\sigma(t)$
$u_{ABS}(t) = \frac{1}{\gamma(t)}\left[-k_1\left(z_2(t) - c_1 z_1(t)\right) - \phi(t) - \hat{\epsilon}(t) + \ddot{y}_d - \dot{\alpha}_1\right] + \frac{1}{\gamma(t)}\left[-h\left(\sigma(t) + \beta sgn\left(\sigma(t)\right)\right)\right]$
return $u_{ABS}(t)$

Fig. 4. Algorithm of the ABSMC method.

3.2 Decoupled Adaptive Backstepping Sliding Mode Control

The ABSMC design is able to be utilized on systems that may be described in the canonical form and it cannot be applied to UMSs directly. Consider a fourth-order underactuated nonlinear system with single input and 2 DOF as follows:

$$\begin{aligned}
\dot{x}_1(t) &= x_2(t) \\
\dot{x}_2(t) &= \phi_1(x,t) + \gamma_1(x,t)u(t) + \epsilon_1(t) \\
\dot{x}_3(t) &= x_4(t) \\
\dot{x}_4(t) &= \phi_2(x,t) + \gamma_2(x,t)u(t) + \epsilon_2(t) \\
y_1(t) &= x_1 \\
y_2(t) &= x_3
\end{aligned} \tag{30}$$

where $x = [x_1, x_2, x_3, x_4]^T$ is the state vector; $y = [y_1, y_2]^T$ is the output; $\phi_1(x,t)$, $\gamma_1(x,t)$, $\phi_2(x,t)$,and $\gamma(x,t)$ are nonlinear functions; $u(t)$ is the control input, and, $\epsilon_1(t)$ and $\epsilon_2(t)$ are the sum of the unmatched uncertainties and external disturbances.

To design an SMC law for an underactuated system such as described in (30), the DSMC approach can be used (Ata and Coban, 2019; Lo and Kuo, 1998). The key concept of the DSMC is decoupling the UMSs into two different subsystems and controlling both sub-systems simultaneously using only one control input. A DABSMC law for UMSs can be designed using the presented ABSMC method.

The control objective is to design a DABSMC system for the outputs $y_1(t)$ and $y_2(t)$ of the system to track the desired outputs $y_{d1}(t)$ and $y_{d2}(t)$. Note that the signals $y_{d1}(t)$, $y_{d2}(t)$, and their first two derivatives are available and they are considered as bounded functions of time.

To achieve the control objective, two different tracking errors can be defined. Considering the first tracking error as

$$\begin{aligned} z_1(t) &= y_1(t) - y_{d1}(t) \\ &= x_1(t) - y_{d1}(t) \end{aligned} \tag{31}$$

and time-derivating it yields

$$\dot{z}_1(t) = x_2(t) - \dot{y}_{d1}(t). \tag{32}$$

Defining a stabilising function as

$$\alpha_{D1}(t) = c_{D1} z_1(t) \tag{33}$$

where c_{D1} is a positive constant and letting $x_2(t) = z_2(t) + \dot{y}_{d1}(t) - \alpha_{D1}(t)$ as a virtual controller result in

$$z_2(t) = x_2(t) - \dot{y}_{d1}(t) + \alpha_{D1}(t). \tag{34}$$

Similarly, the second tracking error can be defined as

$$z_3(t) = x_3(t) - y_{d2}(t). \tag{35}$$

The time derivative of the tracking error $z_3(t)$ results in

$$\dot{z}_3(t) = x_4(t) - \dot{y}_{d2}(t). \tag{36}$$

Defining a stabilising function as

$$\alpha_{D2}(t) = c_{D2} z_3(t) \tag{37}$$

where c_{D2} is a positive constant and considering $x_4(t) = z_4(t) + \dot{y}_{d2}(t) - \alpha_{D2}(t)$ as a virtual control, one has

$$z_4(t) = x_4(t) - \dot{y}_{d2}(t) + \alpha_{D2}(t) \tag{38}$$

as shown in Fig. 5. Accordingly, the fourth-order nonlinear system in Fig. 5 can be written as

$$\begin{aligned} \dot{x}_1(t) &= x_2(t) \\ \dot{x}_2(t) &= \phi_1(x,t) + \gamma_1(x,t) z_4(t) + \varepsilon_1(t) \\ \dot{x}_3(t) &= \phi_2(x,t) + \gamma_2(x,t) z_4(t) + \varepsilon_2(t) \\ \dot{x}_4(t) &= u(t) \\ y_1(t) &= x_1 \\ y_2(t) &= x_3 \end{aligned}$$

Also note that an intermediate variable can be defined as $\tilde{\alpha}_{D2}(t) = \alpha_{D2}(t) - \dot{y}_{d2}(t)$ and this variable can step back through the integrator as illustrated in Fig. 5 (Kristic et al., 1995).

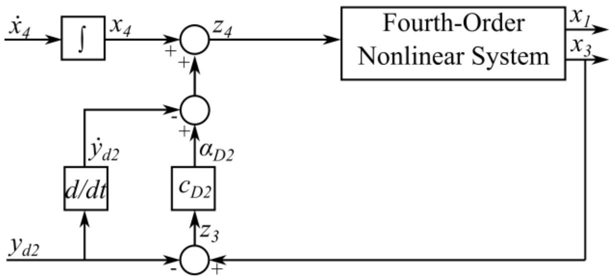

Fig. 5. Introducing the stabilizing function $\alpha_{D2}(t)$ and the error variable $z_4(t)$.

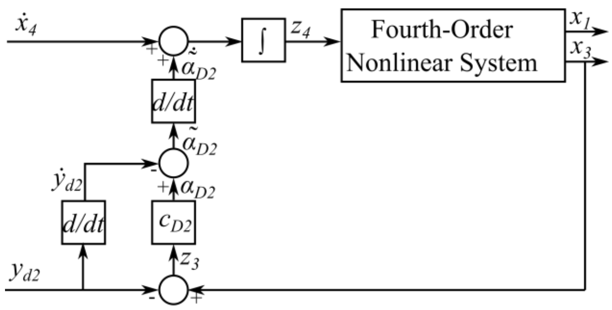

Fig. 6. Backstepping $\tilde{\alpha}_{D2}(t)$ through the integrator.

To design a DABSMC law, the first term of the Lyapunov function candidate can be chosen as

$$V_{D1}(t) = \frac{1}{2} z_3^2(t). \tag{39}$$

The time derivative of the function $V_{D1}(t)$ can be written as

$$\begin{aligned} \dot{V}_{D1}(t) &= z_3(t)\dot{z}_3(t) \\ &= z_3(t)\left(x_4(t) - \dot{y}_{d2}(t)\right) \\ &= z_3(t)\left(z_4(t) - \alpha_{D2}(t)\right) \\ &= z_3(t) z_4(t) - c_{D2} z_3{}^2(t). \end{aligned} \tag{40}$$

In the next step, two different switching functions can be chosen

$$\sigma_{D1}(t) = k_{D1} z_1(t) + z_2(t) \tag{41}$$

and

$$\sigma_{D2}(t) = k_{D2} z_3(t) + z_4(t) \tag{42}$$

where k_{D1} and k_{D2} are positive constants and the Lyapunov function candidate can be extended as

$$V_{D2}(z) = V_{D1}(z) + \frac{1}{2}\sigma_{D2}^2(t). \tag{43}$$

With the help of (30), the time derivative of $z_4(t)$ can be expressed as

$$\begin{aligned}\dot{z}_4(t) &= \dot{x}_4(t) - \ddot{y}_{d2}(t) + \dot{\alpha}_{D2}(t) \\ &= \phi_2(x,t) + \gamma_2(x,t)u(t) + \delta_2(t) - \ddot{y}_{d2}(t) + \dot{\alpha}_{D2}(t).\end{aligned} \quad (44)$$

Using (40) and (44), the time derivative of $V_{D2}(z)$ can be derived as

$$\begin{aligned}\dot{V}_{D2}(z) &= \dot{V}_{D1}(z) + \sigma_{D2}(t)\dot{\sigma}_{D2}(t) \\ &= z_3(t)z_4(t) - c_{D2}z_3^2(t) + \sigma_{D2}(t)\dot{\sigma}_{D2}(t) \\ &= z_3(t)z_4(t) - c_{D2}z_3^2(t) + \sigma_{D2}(t)\left[k_{D2}\dot{z}_3(t) + \dot{z}_4(t)\right] \\ &= z_3(t)z_4(t) - c_{D2}z_3^2(t) + \sigma_{D2}(t)\left[k_{D2}(z_4(t)\right] \\ &\quad +\sigma_{D2}(t)\left[-c_{D2}z_3(t) + \phi_2(x,t) + \gamma_2(x,t)u(t) + \delta_2(t)\right] \\ &\quad +\sigma_{D2}(t)\left[-\ddot{y}_{d2}(t) + \dot{\alpha}_{D2}(t)\right].\end{aligned} \quad (45)$$

The BSMC law can be chosen to guarantee $\dot{V}_{D2}(z)$ is negative definite as follows:

$$\begin{aligned}u_{DBS}(t) &= \frac{1}{\gamma(t)}\left[-k_{D2}(z_4(t) - c_{D2}z_3(t) - \phi_2(t)\right] \\ &\quad + \frac{1}{\gamma(t)}\left[-\bar{\delta}_2(t)sgn(\sigma_{D2}(t)) + \ddot{y}_{d2}(t) - \dot{\alpha}_{D2}(t)\right] \\ &\quad + \frac{1}{\gamma(t)}\left[-h_D\left(\sigma_{D2}(t) + \beta_D sgn\left(\sigma_{D2}(t)\right)\right)\right]\end{aligned} \quad (46)$$

where h_D and β_D are positive constants and uncertainty $\delta_2(t)$ is assumed to be bounded as $|\delta_2(t)| < \bar{\delta}_2(t)$.

Substituting (46) in (45) results in

$$\begin{aligned}\dot{V}_{D2}(z) &= z_3(t)z_4(t) - c_{D2}z_3^2(t) - h_D\sigma_{D2}^2(t) - h_D\beta_D\,|\sigma_{D2}(t)| \\ &\quad + \delta_2(t)\sigma_{D2}(t) - \bar{\delta}_2(t)\,|\sigma_{D2}(t)| \\ &\le z_3(t)z_4(t) - c_{D2}z_3^2(t) - h_D\sigma_{D2}^2(t) - h_D\beta_D\,|\sigma_{D2}(t)| \\ &\quad + |\sigma_{D2}(t)|\left(|\delta_2(t)| - \bar{\delta}_2(t)\right) \\ &\le z_3(t)z_4(t) - c_{D2}z_3^2(t) - h_D\sigma_{D2}^2(t) - h_D\beta_D\,|\sigma_{D2}(t)|\end{aligned} \quad (47)$$

The derivative of the $V_{D2}(z)$ in (47) may be rearranged as

$$\dot{V}_{D2}(z) = -z^T Q_D z - h_D\beta_D\,|\sigma_{D2}(t)| \le 0. \quad (48)$$

where $z^T = \left[z_3 \quad z_4\right]$ and Q_D is a symmetric matrix as

$$Q_D = \begin{bmatrix} c_{D2} + h_D k_{D2}^2 & h_D k_{D2} - 1/2 \\ h_D k_{D2} - 1/2 & h_D \end{bmatrix}. \quad (49)$$

Noting that

$$\begin{aligned}|Q_D| &= h_D(c_{D2} + h_D k_{D2}^2) - (h_D k_{D2} - 1/2)^2 \\ &= h_D c_{D2} + h_D k_{D2} - 1/4 > 0.\end{aligned} \quad (50)$$

and choosing proper values for the constants h_D, c_{D2}, and, k_{D2} yields all the determinants of principal minors of Q_D being strictly positive. Therefore, according to Sylvester's theorem, it is guaranteed that the symmetric matrix Q_D is positive definite. As a result, $\dot{V}_{D2}(z) < 0$ is guaranteed. According to Barbalat's lemma, since z_3 and z_4 converge to 0 as t tends to infinity, the asymptotic stability of the BSMC system is assured.

In the BSMC law proposed in (46), the uncertainty $\delta_2(t)$ is assumed to be bounded as $|\delta_2(t)| < \bar{\delta}_2(t)$. Since it is difficult to determine the upper bound of the uncertainty $\bar{\delta}_2(t)$, an adaptation law can be proposed as

$$\tilde{\delta}_2(t) = \delta_2(t) - \hat{\delta}_2(t) \quad (51)$$

where $\tilde{\delta}_2(t)$ is estimation error and $\hat{\delta}_2(t)$ is estimation. To design an ABSMC law, a new candidate Lyapunov function may be selected as

$$V_{D3}(z) = V_{D2}(z) + \frac{1}{2\xi_D}\tilde{\delta}_2^2(t) \quad (52)$$

where ξ_D is a positive constant. Using the adaptive law proposed in (51) and noting $\dot{\tilde{\delta}}_2(t) = \dot{\delta}_2(t) - \dot{\hat{\delta}}_2(t) = -\dot{\hat{\delta}}_2(t)$, the time derivative of $V_{D3}(z)$ can be derived as

$$\begin{aligned}\dot{V}_{D3}(z) &= \dot{V}_{D2}(z) + \frac{1}{\xi_D}\tilde{\delta}_2(t)\dot{\tilde{\delta}}_2(t) \\ &= z_3(t)z_4(t) - c_{D2}z_3^2(t) \\ &\quad +\sigma_{D2}(t)\left[k_{D2}(z_3(t) - c_{D2}z_3(t))\right] \\ &\quad +\sigma_{D2}(t)\left[\phi_2(x) + \gamma_2(x)u(t) + \delta_2(t) - \ddot{y}_{d2} + \dot{\alpha}_{D2}(t)\right] \\ &\quad -\frac{1}{\xi_D}\tilde{\delta}_2(t)\dot{\hat{\delta}}_2(t) \\ &= z_3(t)z_4(t) - c_{D2}z_3^2(t) + \\ &\quad +\sigma_{D2}(t)\left[k_{D2}(z_4(t) - c_{D2}z_3(t))\right] \\ &\quad +\sigma_{D2}(t)\left[\phi_2(x) + \gamma_2(x)u(t) + \hat{\delta}_2(t) - \ddot{y}_{d2} + \dot{\alpha}_{D2}(t)\right] \\ &\quad -\frac{1}{\xi_D}\tilde{\delta}_2(t)\left(\dot{\hat{\delta}}_2(t) - \xi_D\sigma_{D2}(t)\right).\end{aligned} \quad (53)$$

Defining the adaptation law $\dot{\hat{\delta}}_2(t)$ as

$$\dot{\hat{\delta}}_2(t) = \xi_D\sigma_{D2}(t), \quad (54)$$

an ABSMC law can be proposed as

$$\begin{aligned}u_{DABS}(t) &= \frac{1}{\gamma_2(t)}\left[-k_{D2}\left(z_4(t) - c_{D2}z_3(t)\right)\right] \\ &\quad + \frac{1}{\gamma_2(t)}\left[-\phi_2(t) - \hat{\delta}_2(t) + \ddot{y}_{d2} - \dot{\alpha}_{D2}\right] \\ &\quad + \frac{1}{\gamma_2(t)}\left[-h_D\left(\sigma_{D2}(t) + \beta_D sgn\left(\sigma_{D2}(t)\right)\right)\right].\end{aligned} \quad (55)$$

Substituting (55) in (53) yields

$$\dot{V}_{D3}(z) = z_1(t)z_2(t) - c_{D1}z_1^2 - h_D\sigma_{D2}{}^2(t) - h_D\beta_D \mid \sigma_{D2}(t)\mid . \quad (56)$$

The derivative of the $V_{D3}(z)$ in (56) may be rearranged as

$$\dot{V}_{D3}(z) = -z^T Q_{DA} z - h_D\beta_D \mid \sigma_{D2}(t) \mid \leq 0 \quad (57)$$

where $z^T = \begin{bmatrix} z_3 & z_4 \end{bmatrix}$ and Q_{DA} is a symmetric matrix as

$$Q_{DA} = \begin{bmatrix} c_{D2} + h_D k_{D2}^2 & hk_{D2} - 1/2 \\ h_D k_{D2} - 1/2 & h_D \end{bmatrix}. \quad (58)$$

Similar to (50), choosing proper values for the constants h_D, c_{D2}, and, k_{D2} guarantees the symmetric matrix Q_{DA} is positive definite. It indicates that the asymptotic stability of the system is ensured by using the ABSMC according to Barbalat's lemma.

To design a DASMC law, the switching function $\sigma_{D2}(t)$ in (42) can be reconstructed as a decoupled function as

$$\sigma_{DS}(t) = k_{D2}(z_3(t) - z_D(t)) + z_4 \quad (59)$$

where $z_D(t)$ is a value transferred from $\sigma_{D1}(t)$ in (41). The intermediate variable $z_D(t)$ can be defined as

$$z_D(t) = sat\left(\frac{\sigma_{D1}(t)}{\Delta_D}\right) z_U \quad (60)$$

where z_U is the upper bound of $z_D(t)$ as a constant bounded $0 < z_U < 1$, Δ_D is the boundary level as a constant, and the saturation function $sat(\eta)$ is

$$sat(\eta) = \begin{cases} sgn(\eta), & \mid \eta \mid \geq 1 \\ \eta, & \mid \eta \mid < 1. \end{cases} \quad (61)$$

z_U ensures $\sigma_{DS}(t)$ will be limited, and when the switching function $\sigma_{D1}(t)$ converges 0, $\sigma_{DS}(t)$ will be driven to zero too, thanks to z_D.

Consequently, replacing the decoupled function σ_{DS} in (59) into (55) gives a DABSMC law for UMSs as

$$\begin{aligned} u_{DABSMC}(t) = &\frac{1}{\gamma_2(t)}\left[-k_{D2}\left(z_4(t) - c_{D2}z_3(t)\right)\right] \\ &+ \frac{1}{\gamma_2(t)}\left[-\phi_2(t) - \hat{\delta}_2(t) + \ddot{y}_{d2} - \dot{\alpha}_{D2}\right] \\ &+ \frac{1}{\gamma_2(t)}\left[-h_D\left(\sigma_{DS}(t) + \beta_D sgn\left(\sigma_{DS}(t)\right)\right)\right] \end{aligned} \quad (62)$$

with the adaptation law

$$\dot{\hat{\delta}}_2(t) = \xi_D \sigma_{DS}(t). \quad (63)$$

The design steps of the proposed DABSMC method are summarized in Fig. 7.

Input : **System states** $x_1(t)$, $x_2(t)$, $x_3(t)$ and $x_4(t)$;
System functions $\phi_2(t)$, $\gamma_2(t)$;
External disturbance $\epsilon_2(t)$;
Desired outputs $y_{d1}(t)$ and $y_{d2}(t)$;
Controller parameters c_{D1}, c_{D2}, k_{D1}, k_{D2}, ξ_D, h_D, β_D, Δ_D and z_U

Output: **The DABSMC output** $u_{DABSMC}(t)$

$z_1(t) = x_1(t) - y_{d1}(t)$
$\alpha_{D1}(t) = c_{D1}z_1(t)$
$z_2(t) = x_2(t) - \dot{y}_{d1}(t) + \alpha_{D1}(t)$
$z_3(t) = x_3(t) - y_{d2}(t)$
$\alpha_{D2}(t) = c_{D2}z_3(t)$
$z_4(t) = x_4(t) - \dot{y}_{d2}(t) + \alpha_{D2}(t)$
$V_{D1}(t) = \frac{1}{2}z_3^2(t)$
$\sigma_{D1}(t) = k_{D1}z_1(t) + z_2(t)$
$\sigma_{D2}(t) = k_{D2}z_3(t) + z_4(t)$
$V_{D2}(z) = V_{D1}(z) + \frac{1}{2}\sigma_{D2}{}^2(t)$
$\tilde{\epsilon}_2(t) = \epsilon_2(t) - \hat{\epsilon}_2(t)$
$\dot{\tilde{\epsilon}}_2(t) = \dot{\epsilon}_2(t) - \dot{\hat{\epsilon}}_2(t) = -\dot{\hat{\epsilon}}_2(t)$
$V_{D3}(z) = V_{D2}(z) + \frac{1}{2\xi}\tilde{\epsilon}_2{}^2(t)$
$z_D(t) = sat\left(\frac{\sigma_{D1}(t)}{\Delta_D}\right) z_U$
$\sigma_{DS}(t) = k_{D2}(z_3(t) - z_D(t)) + z_4$
$\dot{\hat{\epsilon}}_2(t) = \xi\sigma_{DS}(t)$
$$\begin{aligned} u_{DABSMC}(t) = &\frac{1}{\gamma_2(t)}\left[-k_{D2}\left(z_4(t) - c_{D2}z_3(t)\right)\right] \\ &+ \frac{1}{\gamma_2(t)}\left[-\phi_2(t) - \hat{\epsilon}_2(t) + \ddot{y}_{d2} - \dot{\alpha}_{D2}\right] \\ &+ \frac{1}{\gamma_2(t)}\left[-h_D\left(\sigma_{DS}(t) + \beta_D sgn\left(\sigma_{DS}(t)\right)\right)\right] \end{aligned}$$
return $u_{DABSMC}(t)$

Fig. 7. Algorithm of the DABSMC method.

4. EXPERIMENTAL RESULTS

The proposed DABSMC scheme is applied to a real IPC system in order to validate performance and robustness of it. Using the control law proposed in (62) a DABSMC law for the IPC system introduced in (4) can be designed. Since the control object is defined as stabilizing the pendulum in the vertical position while bringing the cart to the desired position; tracking errors $z_1(t)$ and $z_3(t)$ may be defined as $z_1(t) = x - y_{d1}(t)$ and $z_3(t) = \theta - y_{d2}(t)$, respectively. Also, a saturation function can be employed in (62) instead of the signum function to avoid chattering. Eventually, a DABSMC law for the IPC system introduced in (4) is given by

$$\begin{aligned} u_{DABSMC}(t) = &\frac{1}{\gamma_2(t)}\left[-k_{D2}\left(z_4(t) - c_{D2}z_3(t)\right)\right] \\ &+ \frac{1}{\gamma_2(t)}\left[-\phi_2(t) - \hat{\delta}_2(t) + \ddot{y}_{d2}\right] \\ &+ \frac{1}{\gamma_2(t)}\left[-\dot{\alpha}_{D2} - h_D\left(\sigma_{DS}(t) + \beta_D sat\left(\sigma_{DS}(t)\right)\right)\right] \end{aligned} \quad (64)$$

with the adaptation law

$$\dot{\hat{\delta}}_2(t) = \xi_D \sigma_{DS}(t) \quad (65)$$

where

$$\phi_2(t) = \frac{\omega_2\left(a_{n5}x_2\cos(x_3) + a_{n6}\sin(x_3) + a_{n7}x_4\right)}{a_{m1} - a_{m2}\cos^2(x_3)} + \frac{\omega_2 a_{n8}\cos(x_3)\sin(x_3)x_4^2}{a_{m1} - a_{m2}\cos^2(x_3)}$$

and

$$\gamma_2(t) = \frac{a_{n9}\cos(x_3)}{a_{m1} - a_{m2}\cos^2(x_3)}.$$

The proposed control method is experimentally compared with the DSMC method (Coban and Ata, 2017). To design a DSMC law for the IPC system, the first switching function $\sigma_{S1}(t)$ can be defined as

$$\sigma_{S1}(t) = m_1(x_1(t) - y_{d1}) + (\dot{x}_1(t) - \dot{y}_{d1}) \tag{66}$$

where m_1 is a positive constant. Based on $\sigma_{S1}(t)$, the intermediate variable $z_S(t)$ can be defined as

$$z_S(t) = sat(\sigma_{S1}(t)/\Delta_S)z_{US} \tag{67}$$

where Δ_S is the boundary level and z_{US} is the upper bound of z_S as constants. The decoupled switching function $\sigma_{S2}(t)$ can be constructed using $z_S(t)$ as

$$\sigma_{S2}(t) = m_2\left[(x_3(t) - y_{d2}) - z_S(t)\right] + (\dot{x}_3(t) - \dot{y}_{d2}) \tag{68}$$

where m_2 is a positive constant. Consequently, the DSMC law for the IPC system can be designed as follows (Coban and Ata, 2017):

$$u_S(t) = \frac{1}{\gamma_2(x,t)}\left[-m_2\dot{z}_3(t) - \phi_2(x,t) - Ksat(\sigma_{S2})\right] \tag{69}$$

where K is a positive constant.

The experimental tests are carried out on Feedback Instrument's digital pendulum system (Feedback Instruments, 2006a). The experimental setup and the block diagram of the proposed control system are presented in Fig. 8. and Fig. 9, respectively. A PCI 1711 Advantech card installed PC serves as the main control unit on the experimental setup. The control signal is transferred to the Digital Pendulum Controller (DPC) using a Digital Analog Converter (DAC). The pendulum angle and the cart position signals are transferred to the DPC and then to the PC by an Encoder. The sample times of the DAC and Encoder are set as $0.001s$ by default (Feedback Instruments, 2006b).

The selected control task consists in maintaining the stability of the pendulum in the upward position while moving the cart to the desired position. During the experiments, total parametric uncertainties of the system are considered as ω_2 and no external perturbation is added into the system. For all experiments, the initial conditions are selected as $[x_0\ \dot{x}_0\ \theta_0\ \dot{\theta}_0]^T = [0\ 0\ 0.1\ 0]^T$. The expected outputs of the cart position and the pendulum angle are selected as $y_{d1} = 0.3m$ and $y_{d2} = 0rad$, respectively. Since the values of the desired outputs, y_{d1} and y_{d2} are constants their first and second derivatives with respect to the time are available and considered as 0.

Fig. 8. The IPC system.

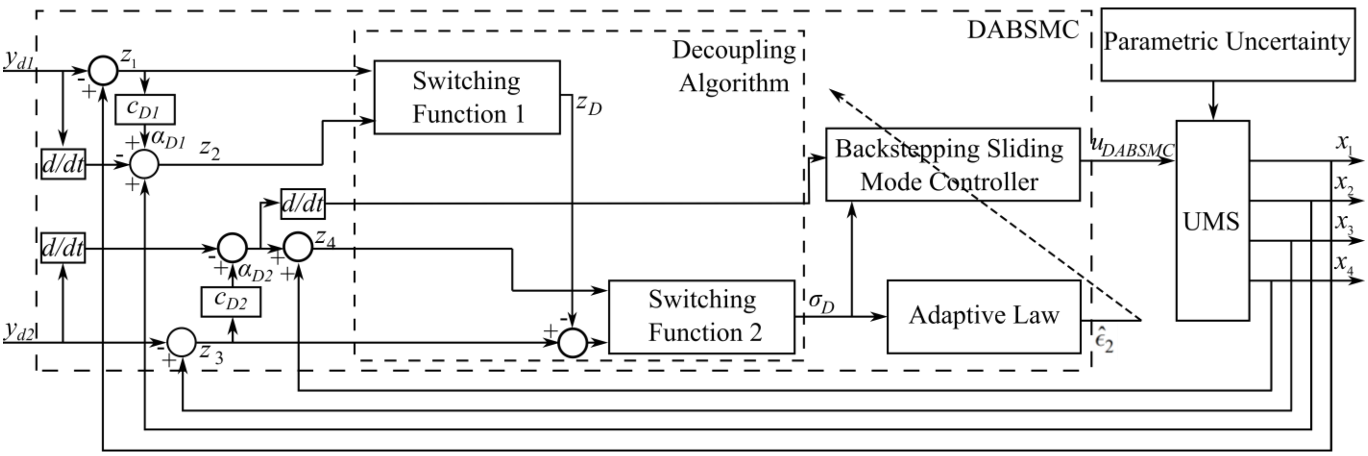

Fig. 9. Block diagram of the proposed controller.

The DABSMC parameters are chosen as $c_{D1} = 0.2$, $c_{D2} = 4$, $k_{D1} = 0.5$, $k_{D2} = 40$, $\xi_D = 1$, $h_D = 10$, $\beta_D = 3$, $z_U = 0.97$ and $\Delta_D = 6$ using the trial-and-error method with considering the best likely performances in terms of tracking error and response time. Also, the DSMC parameters are selected as $m_1 = 1$, $m_2 = 40$, $K = 30$, $z_{US} = 0.97$ and

$\Delta_S = 6$ to achieve the best control performance considering the tracking error and response time by trial-and-error. The IPC system with DC motor parameters are considered as follows: $M = 2.3kg$, $b = 0.00005Ns/m$, $m = 0.2kg$, $l = 0.3m$, $d = 0.005Nms/rad$, $I = 0.009kgm^2$, $g = 9.81m/s^2$, $K_b = 0.05$, $K_t = 0.05$, $R = 2.5\Omega$, $n_1 = 18.84$, $n_2 = 0.986$, and, $r = 0.0314m$ (Ata and Coban, 2017; Feedback Instruments, 2006a)

In the first test, both the DSMC and the DABSMC methods are applied to the IPC system with $\omega_2 = 1$. Thus, no additional parametric uncertainty is added into the system and the test is carried out on the own parametric uncertainties of the IPC system. The cart position, pendulum angle, and control input for both methods are presented in Fig. 10, Fig. 11, and Fig. 12, respectively.

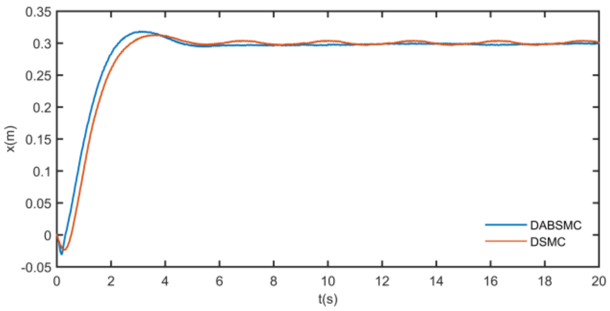

Fig. 10. Linear displacement with the parametric uncertainty $\omega_2 = 1$.

In the second test, both the DSMC and the DABSMC methods are applied to the IPC system with the parametric uncertainty $\omega_2 = 0.8$. The cart position, pendulum angle, and control input for both methods are presented in Fig. 13, Fig. 14, and Fig. 15, respectively.

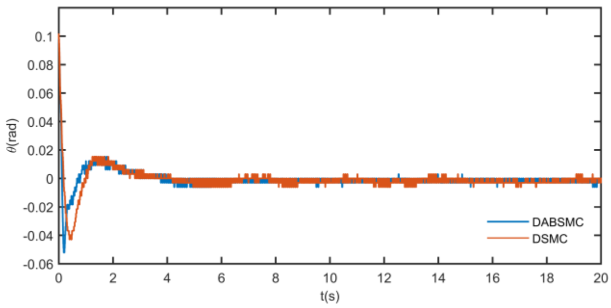

Fig. 11. Angular displacement with the parametric uncertainty $\omega_2 = 1$.

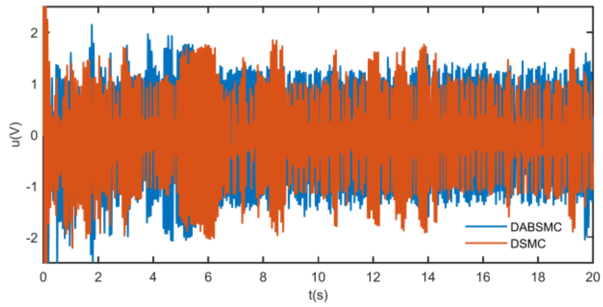

Fig.12. Control signal with the parametric uncertainty $\omega_2 = 1$.

Both the DABSMC and the DSMC methods are managed to control the pendulum on the vertical position as shown in Fig. 11. However, the chattering in the control input is slightly higher in the DABSMC as shown in Fig. 12.

Table 1. The DSMC/DABSMC performance ratios.

Tracking Error	IAE	ISE	ITAE	ITSE
Cart Position (m)	1.148	1.266	1.129	1.466
Pendulum Angle (rad)	1.134	1.248	1.094	1.26
Control Signal (V)	0.889	0.854	0.863	0.825

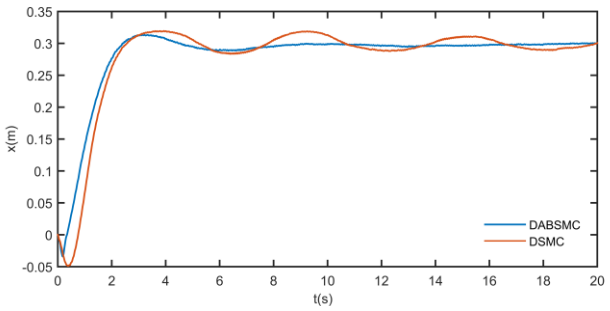

Fig. 13. Linear displacement with the parametric uncertainty $\omega_2 = 0.8$.

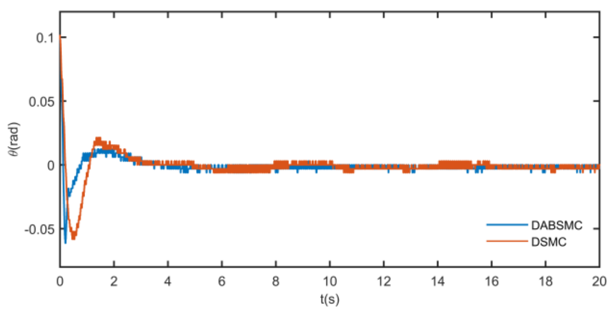

Fig. 14. Angular displacement with the parametric uncertainty $\omega_2 = 0.8$.

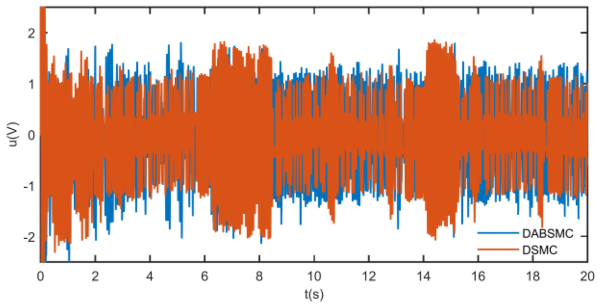

Fig. 15. Control signal with the parametric uncertainty $\omega_2 = 0.8$.

Fig. 14 clearly shows that the DSMC can stabilize the pendulum at the vertical position but it completely fails to manage to stabilise the cart at the desired position as presented in Fig. 13. Contrarily, the DABSMC overcomes the parametric uncertainty and manages to control the cart position at 6.657 s settling time with 4.457 percent overshoot and 11.349 percent undershoot. However, it cost lightly higher chattering in the control signal as shown in Fig. 15.

The performance of the controllers can also be measured by the performance indices which use the tracking error with the evaluation time, generally. Some of the error-based performance indices are formulated as follows:

- Integral Squared Error (ISE): $\int_0^T e^2(t)dt$
- Integral Time Squared Error (ITSE): $\int_0^T te^2(t)dt$
- Integral Absolute Error (IAE): $\int_0^T |e(t)|\, dt$
- Integral Time Absolute Error (ITAE): $\int_0^T t\,|e(t)|\, dt$

where t is time bounded as $t < T$ and $e(t)$ is the tracking error. The experimental tests are carried out for $20s$. Hence, T is considered as $20s$ in performance indices analysis. The DSMC/DABSMC performance ratios based on performance indices with parametric uncertainty $\omega_2 = 1$ are given in Table 1. The magnitudes of all performance indices for cart position and pendulum angle are smaller in the DABSMC rather than the DSMC as shown in Table 1. Consequently, the DABSMC produced a more accurate control input than the DSMC.

5. CONCLUSIONS

In this paper, the design and implementation of a decoupled adaptive backstepping sliding mode control (DABSMC) approach are presented to control 2 degrees of freedom underactuated mechanical systems subject to parametric uncertainties and external disturbances. The proposed DABSMC method keeps the merits of the adaptive backstepping control and sliding mode control to design a robust controller against the parametric uncertainties. Moreover, it can be directly applied to underactuated mechanical systems due to its decoupling nature. The effectiveness and robustness of the proposed DABSMC are confirmed by experimental tests on a real-life inverted pendulum on a cart system. The experimental results justify the satisfying performance of the proposed method. Also, the experiments show that the proposed DABSMC approach presents robustness against the parametric uncertainties compared to the conventional decoupled sliding mode control.

REFERENCES

Adhikary, N., and Mahanta, C. (2013). Integral backstepping sliding mode control for underactuated systems: Swing-up and stabilization of the Cart-Pendulum System. *ISA Transactions*, *52*(6), 870–880.

Anderson, C. W. (1988). Learning to Control an Inverted Pendulum Using Neural Networks. *1988 American Control Conference, April*, 2294–2298.

Åström, K. J., and Furuta, K. (2000). Swinging up a pendulum by energy control. *Automatica*, *36*(2), 287–295.

Ata, B., and Coban, R. (2017). Linear Quadratic Optimal Control of an Inverted Pendulum on a Cart using Artificial Bee Colony Algorithm: An Experimental Study. *Cukurova University Journal of the Faculty of Engineering and Architecture*, *32*(2), 109–124.

Ata, B., and Coban, R. (2019). Decoupled Backstepping Sliding Mode Control of Underactuated Systems with Uncertainty: Experimental Results. *Arabian Journal for Science and Engineering*, *44*(8), 7013–7021.

Chang, W.-D., Hwang, R.-C., & Hsieh, J.-G. (2002). A self-tuning PID control for a class of nonlinear systems based on the Lyapunov approach. *Journal of Process Control*, *12*(2), 233–242.

Coban, R. (2017). Dynamical adaptive integral backstepping variable structure controller design for uncertain systems and experimental application. *International Journal of Robust and Nonlinear Control*, *27*(18), 4522–4540.

Coban, R. (2019). Adaptive backstepping sliding mode control with tuning functions for nonlinear uncertain systems. *International Journal of Systems Science*, *50*(8), 1517–1529.

Coban, R., and Ata, B. (2017). Decoupled sliding mode control of an inverted pendulum on a cart: An experimental study. *2017 IEEE International Conference on Advanced Intelligent Mechatronics (AIM)*, 993–997.

Deng, L., and Gao, S. (2011). The design for the controller of the linear inverted pendulum based on backstepping. *Proceedings of 2011 International Conference on Electronic & Mechanical Engineering and Information Technology*, 2892–2895.

Dong, L., and Tang, W. C. (2014). Adaptive backstepping sliding mode control of flexible ball screw drives with time-varying parametric uncertainties and disturbances. *ISA transactions*, *53*(1), 110–116.

Fantoni, I., and Lozano, R. (2002). *Non-linear Control for Underactuated Mechanical Systems*. Springer London.

Feedback Instruments (2006a). 33-936S Digital Pendulum

Control Experiments Manual.

Feedback Instruments (2006b). 33-936IC Digital Pendulum Installation & Commissioning Manual.

Freeman, R. A., and Kokotović, P. (1996). *Robust Nonlinear Control Design*. Birkhäuser Boston.

Ge, S. S., Hang, C. C., Lee, T. H., and Zhang, T. (2002). *Stable Adaptive Neural Network Control*. Springer US.

Huang, X., Ralescu, A. L., Gao, H., and Huang, H. (2019). A survey on the application of fuzzy systems for underactuated systems. *Proceedings of the Institution of Mechanical Engineers, Part I: Journal of Systems and Control Engineering*, *233*(3), 217–244.

Hussein, I. I., and Bloch, A. M. (2008). Optimal control of underactuated nonholonomic mechanical systems. *IEEE Transactions on Automatic Control*, *53*(3), 668–682.

Isidori, A. (1995). *Nonlinear Control Systems*. Springer London.

Jeong, S. H., and Takahashi, T. (2007). Wheeled Inverted PENdulum Type Assistant Robot: Inverted mobile, standing, and sitting motions. *IEEE International Conference on Intelligent Robots and Systems*, 1932–1937.

Kanellakopoulos, I., Kokotovic, P. V., and Morse, A. S. (1991). Systematic design of adaptive controllers for feedback linearizable systems. *Proceedings of the American Control Conference*, *1*, 649–654.

Kennedy, E., King, E., and Tran, H. (2019). Real-time implementation and analysis of a modified energy based controller for the swing-up of an inverted pendulum on a cart. *European Journal of Control*, *50*, 176–187.

Koshkouei, A. J., and Zinober, A. S. I. (2000). Adaptive backstepping control of nonlinear systems with unmatched uncertainty. *Proceedings of the 39th IEEE Conference on Decision and Control*, *5*(4), 4765–4770.

Kristic, M., Kanellakopoulos, I., and Kokotovic, P. (1995). *Nonlinear and Adaptive Control Design*. Wiley.

Kuo, A. D. (2007). The six determinants of gait and the inverted pendulum analogy: A dynamic walking perspective. *Human Movement Science*, *26*(4), 617–656.

Lee, H., and Utkin, V. I. (2007). Chattering suppression methods in sliding mode control systems. *Annual Reviews in Control*, *31*(2), 179–188.

Lin, F.-J., Shen, P.-H., and Hsu, S.-P. (2002). Adaptive backstepping sliding mode control for linear induction motor drive. *IEE Proceedings - Electric Power Applications*, *149*(3), 184.

Liu, S. Q., Sang, Y. J., and Whidborne, J. F. (2020). Adaptive sliding-mode-backstepping trajectory tracking control of underactuated airships. *Aerospace Science and Technology*, *97*, 105610.

Liu, Y., and Yu, H. (2013). A survey of underactuated mechanical systems. *IET Control Theory and Applications*, *7*(7), 921–935.

Lo, J.-C., and Kuo, Y.-H. (1998). Decoupled fuzzy sliding-mode control. *IEEE Transactions on Fuzzy Systems*, *6*(3), 426–435.

Ma, L., Schilling, K., and Schmid, C. (2006). Adaptive Backstepping Sliding-Mode Control With Application To A Flexible-Joint Manipulator. *IFAC Proceedings Volumes*, *39*(16), 55–60.

Mahjoub, S., Mnif, F., and Derbel, N. (2015). Second-order sliding mode approaches for the control of a class of underactuated systems. *International Journal of Automation and Computing*, *12*(2), 134–141.

Olfati-Saber, R. (2001). *Nonlinear Control of Underactuated Mechanical Systems with Application to Robotics and Aerospace Vehicles*. Massachusetts Institute Of Technology.

Oryschuk, P., Salerno, A., Al-Husseini, A. M., and Angeles, J. (2009). Experimental validation of an underactuated two-wheeled mobile robot. *IEEE/ASME Transactions on Mechatronics*, *14*(2), 252–257.

Reyhanoglu, M., Van Der Schaft, A., McClamroch, N. H., and Kolmanovsky, I. (1999). Dynamics and control of a class of underactuated mechanical systems. *IEEE Transactions on Automatic Control*, *44*(9), 1663–1671.

Saco, R. (2019). Subspace Identification of an Inverted Pendulum on a Cart using State Variables Transformation. *IFAC-PapersOnLine*, *52*(11), 244–249.

Siuka, A., and Schöberl, M. (2009). Applications of energy based control methods for the inverted pendulum on a cart. *Robotics and Autonomous Systems*, *57*(10), 1012–1017.

Slotine, J.-J., and Li, W. (1991). *Applied NoLinear Optimal Control*. Prentice Hall.

Spong, M. W. (1987). Modeling and Control of Elastic Joint Robots. *Journal of Dynamic Systems, Measurement, and Control*, *109*(4), 310.

Spong, Mark W. (1998). Underactuated mechanical systems. *Control Problems in Robotics and Automation, Springer*, 135–150.

Subudhi, B., Ghosh, A., and Krishnan, T. R. (2012). Robust proportional–integral–derivative compensation of an inverted cart–pendulum system: an experimental study. *IET Control Theory & Applications*, *6*(8), 1145–1152.

Utkin, V. (1977). Variable structure systems with sliding modes. *IEEE Transactions on Automatic Control*, *22*(2), 212–222.

Utkin, Vadim. (1992). *Sliding Modes in Control and Optimization*. Springer Berlin Heidelberg.

Walsh, G. C., Montgomery, R., and Sastry, S. S. (1994). Orientation control of the dynamic satellite. *Proceedings of 1994 American Control Conference - ACC '94*, *1*, 138–142.

Woods, S. A., Bauer, R. J., and Seto, M. L. (2012). Automated ballast tank control system for autonomous underwater vehicles. *IEEE Journal of Oceanic Engineering*, *37*(4), 727–739.

Wu, J., and Lu, Y. (2019). Adaptive Backstepping Sliding Mode Control for Boost Converter With Constant Power Load. *IEEE Access*, *7*, 50797–50807.